Research and Development of Imaging Bolometers

Byron J. PETERSON, Shigeru KONOSHIMA[1)], Artem Yu. KOSTRYUKOV[2)], Dongcheol SEO[3)], Yi LIU, Igor V. MIROSHNIKOV[2)], Naoko ASHIKAWA, Homaira PARCHAMY, Hisato KAWASHIMA[1)], Naofumi IWAMA[4)], Masashi KANEKO, the LHD team and the JT-60U team[1)]

NIFS, Toki-shi, Gifu-ken 509-5292, Japan
[1)]*JAEA, Naka-machi, Ibaraki-ken 311-0193, Japan*
[2)]*St. Petersburg State Tech. Univ., St. Petersburg 195251, Russia*
[3)]*National Fusion Research Center, Daejeon 305-806, Korea*
[4)]*Daido Inst. Tech., Nagoya 457-8530, Japan*

(Received 4 December 2006 / Accepted 13 March 2007)

An overview of the research and development of imaging bolometers giving a perspective on the applicability of this diagnostic to a fusion reactor is presented. Traditionally the total power lost from a high temperature, magnetically confined plasma through radiation and neutral particles has been measured using one dimensional arrays of resistive bolometers. The large number of signal wires associated with these resistive bolometers poses hazards not only at the vacuum interface, but also in the loss of electrical contacts that has been observed in the presence of fusion reactor levels of neutron flux. Imaging bolometers, on the other hand, use the infrared radiation from the absorbing metal foil to transfer the signal through the vacuum interface and out from behind a neutron shield. Recently a prototype imaging bolometer known as the InfraRed imaging Video Bolometer has been deployed on the JT-60U tokamak which demonstrates the ability of this diagnostic to operate in a reactor environment. The application of computed tomography demonstrates the ability of one imaging bolometer with a semi-tangential view to produce images of the plasma emissivity. In addition, new detector foil development promises to strengthen the foil and increase the sensitivity by an order of magnitude.

Keywords: bolometer, infrared camera, fusion reactor, imaging, plasma diagnostics, plasma radiation, computed tomography

DOI: 10.1585/pfr.2.S1018

1. Introduction

The ultimate objective of bolometer diagnostics in fusion research is to provide spatially and temporally resolved measurements of total (broad band) radiated power loss (and also losses from neutral particles) from a high temperature plasma. Typically this objective has been realized by multiple one dimensional arrays of resistive bolometers arranged around one poloidal cross-section (constant toroidal angle) [1, 2]. A tomographic inversion is employed to produce from the line-averaged signals an image of the plasma radiation intensity in that cross-section, which in the case of a tokamak can be considered representative of the entire plasma due to the inherent toroidal symmetry.

The resistive bolometers widely used consist of thin (typically 4 μm) gold (Au) or platinum (Pt) foil absorbers which are electrically isolated from a grid of the same material by a kapton or mica insulating layer [3]. The foil absorbs the incoming radiation through an aperture, then the resulting heat is transferred through the insulating layer to the grid. The change in temperature of the grid results in a change in its resistance which is sensed using an electrical circuit. Two measuring and two reference grids are arranged in a wheatstone bridge circuit, therefore each detector requires 4 sensing wires and a ground or 5 electrical feedthroughs through the vacuum interface.

Experience with tokamak operation and tests on a nuclear reactor have shown that these resistive bolometers may not be durable enough for a fusion reactor. In particular the electrical connections have been shown to be susceptible to failure due to the thermal stresses encountered during irradiation with neutrons at fusion reactor levels [4]. In addition electronic drift of the signal due to uncompensated changes in the temperature of the surrounding foil housing poses problems for steady state measurement. Therefore research and development of resistive bolometers continues in an effort to find a reactor relevant solution.

An alternative to the resistive bolometer has been proposed [5] and has evolved into a device called the infrared imaging video bolometer (IRVB) [6, 7]. This concept relies on a single, large (typically 7 cm × 9 cm), thin (1-5 μm), Au (or some other suitable material) foil held in a copper

author's e-mail: peterson@LHD.nifs.ac.jp

frame, exposing one surface of the foil to the plasma radiation through an aperture and one surface through a vacuum IR window to an infrared camera located outside the vacuum vessel. The change in the temperature of the foil due to the absorption of the photon energy from the plasma is measured by the infrared camera. The two-dimensional (2D) heat diffusion equation of the foil is solved to derive the radiated power density absorbed by the foil from the 2D temperature profile on the foil, providing a 2D image of the plasma radiation. The advantage of this concept relative to the resistive bolometers is the lack of wires and electrical contacts and the suitability of the materials to a reactor environment. Also, electronic signal drift is avoided as the foil temperature is measured with respect to the surrounding frame, which is also being constantly measured, and therefore the effect of the heating of the surrounding structure is automatically compensated in the analysis. Therefore IRVBs are better suited to measurement of radiation in a steady state fusion reactor than conventional resistive bolometers. Several IRVBs have been installed and operated on the Large Helical Device [8, 9]. In JT-60U a prototype IRVB has been installed and operated demonstrating the ability of this device to operate in a tokamak reactor environment [10, 11]. In addition calibration techniques have been developed [7, 12, 13]. In this paper we investigate the sensitivity of the IRVB in terms of IR camera performance in Section 2. In Section 3 we discuss the choice of foil materials. In Section 4 we demonstrate for the first time the ability of an IRVB with a semi-tangential view to produce an image of the 2D plasma radiation profile using computed tomography. In Section 5 we discuss the impact that the development of a new double layer foil will have on the sensitivity of the diagnostic. In Section 6 plans for an upgrade of the JT-60U IRVB are introduced. Finally in Section 7 we will summarize with a perspective on the future applicability of this diagnostic to a fusion reactor.

2. IR Camera Performance and IRVB Sensitivity

The noise equivalent power for the IRVB has been previously derived [7] and we rewrite this as the noise equivalent power density, S_{IRVB}, (by dividing by the bolometer pixel area)

$$S_{IRVB} = \frac{\eta_{IRVB} N_{bol}}{A_f} = \frac{\sqrt{2} k t_f \sigma_{IR}}{\sqrt{f_{IR} N_{IR}}} \sqrt{\frac{5 N_{bol}^3 f_{bol}}{A_f^2} + \frac{N_{bol} f_{bol}^3}{\kappa^2}} \quad (1)$$

in terms of the IR camera parameters: sensitivity, σ_{IR}, frame rate, f_{IR}, and number of pixels, N_{IR}, the foil properties: area, A_f, thickness, t_f, thermal conductivity, k, and thermal diffusivity, κ, and the IRVB parameters: frame rate, f_{bol} and number of channels, N_{bol}. The blackbody radiation term is not included since it is negligible for background temperatures below 1000 K. In Table 1 the performance parameters of commercially available IR cameras and the resulting S_{IRVB} are shown. In Figure 1 S_{IRVB} is plotted versus N_{bol}. This shows the trade off that is made between the number of IRVB channels (which corresponds to spatial resolution) and sensitivity. Above approximately 640 channels the noise is dominated by the Laplacian term (left hand term under radical in Eq. 1), while below 640 channels it is dominated by the time derivative term (right hand term under radical in Eq. 1). Both Table 1 and Figure 1 show clearly the improvement that can be made in the sensitivity of the IRVB with a high performance IR camera. It should be noted that the values of σ_{IR} are nominal values and in many cases can be reduced by improving the optics. For instance with the Omega camera we achieved a

Table 1 Performance parameters of IR cameras and the resulting S_{IRVB} for a gold IRVB foil with N_{bol} = 192, A_f = 60.75 cm^2, t_f = 4 μm, f_{bol} = 30/s (S-Sterling, μbolo-microbolometer, FPA-focal plane array).

Maker/ model	FLIR/ Omega	FLIR/ SC500	FLIR/ A40-M	FLIR/ Phoenix	FLIR/ SC4000	FLIR/ SC6000
Wave length (μm)	7.5-13.5	7.5-13	7.5-13	3-5	3-5	3-5
σ_{IR} (m℃@ 30℃)	100	100	80	25	25	25
detector type	FPA μbolo	FPA μbolo	FPA μbolo	FPA InSb	FPA InSb	FPA InSb
cooling	none	none	none	S	S	S
N_{IR}	160x120	320x240	320 x 240	320 x 256	320 x 256	640 x 512
f_{IR} (Hz)	30	60	60	345	420	125
S_{IRVB} (μW/cm^2)	441	156	125	16	14	13

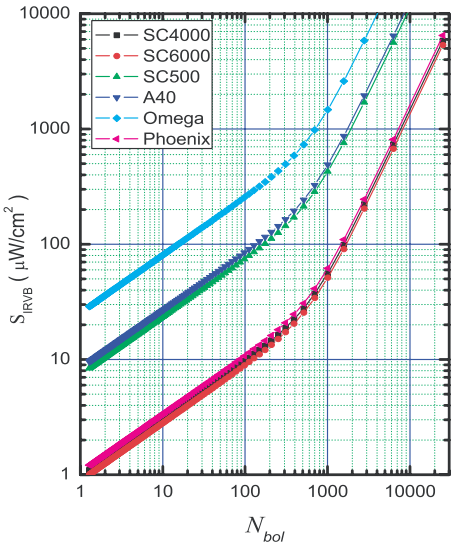

Fig. 1 S_{IRVB} versus N_{bol} for a gold IRVB foil with A_f = 60.75 cm^2, t_f = 4 μm, f_{bol} = 30/s for 6 different IR cameras.

bit equivalent noise of 67 mC which is 67 % of the nominal value.

3. Foil Material Choice

Many considerations should be taken in the choice of the foil material. A detailed study of this was made earlier [14], but several additional considerations should be made at this time based on past results. In Table 2 the parameters for 5 foil materials are shown. Each of these metals have a large stopping cross-section for energetic photons which is expressed in terms of the minimum photon energy, E_{ph}, that can be stopped by a 10 μm foil. Also their high melting temperatures, T_m, insure that they can survive the high temperatures at the reactor vessel wall. In terms of sensitivity (the inverse of S_{IRVB}), when the time derivative term dominates (at high frame rate and low channel number) in Eq. 1, the sensitivity is proportional to κ/k, but when the Laplacian term dominates, then it is inversely proportional to k. In both operating regimes Hafnium (Hf) and Tantalum (Ta) are the most sensitive materials. Another factor to consider is the strength of the material. In JT-60U some motion of the 2.5 μm Au foil was observed prior to and during the discharge. This motion of the foil may be hard to distinguish from changes in the foil temperature due to changes in the reflection of surrounding warm surfaces. This problem may be mitigated in the future by the use of a thicker and stronger foil. Good candidates in this regard are Tungsten (W), Ta and Hf. Another important consideration in terms of a reactor is the neutron cross-section. This is important for the nuclear heating and activation of the foil. Pt, W and Ta are the best in this regard. For high sensitivity in the regime dominated by the Laplacian term sensitivity is proportional to A_f. However, the commercial availability of large thin foils is limited. In Table 2 this is indicated by t_{min}, the minimum thickness available in a 10 cm × 10 cm foil. Considering all of these factors together, for a reactor such a ITER where a 10 μm foil would be necessary, W would be the best material in terms of strength and neutron cross-section. Au is not suitable for a reactor due to its transmutation to mercury in the presence of high neutron fluence [4]. For smaller machines where a thinner foil would be adequate, Ta may be the optimal material due to its higher sensitivity and strength compared to Au and Pt.

Table 2 Parameters of various prospective foil materials [15].

	Tensile strength (MPa) Hard	$\sigma_{neutron}$ (Barns)	k (W/m K) @0-100C	κ/k (cm^3 K/J)	T_m (C)	E_{ph}[16] (keV) @10μm	t_{min} (μm)
Hf	745	103	23.0	0.52	2227	18.4	9
Ta	760	22	57.5	0.43	2996	20.1	2
Au	220	98.8	318	0.40	1064	23.2	2.5
W	1920	18.5	173	0.39	3410	21.4	10
Pt	200-300	9.0	71.6	0.35	1772	23.9	2

4. 2D Emissivity Data from a Semi-tangential IRVB

As was mentioned in the introduction, the objective of a bolometer diagnostic system, particularly in a tokamak, is to provide a spatially and temporally resolved measurement of the radiation emissivity in a poloidal cross-section. Using one imaging bolometer in JT-60U this has been accomplished by means of a computed tomographic reconstruction [17]. In Figure 2 the field of view of the IRVB in JT-60U is shown along with the brightness profile image (corrected by the effective area of each bolometer pixel) for a discharge in JT-60U where significant radiation from the core due to heavy impurity accumulation was observed [11]. In Figure 3 the two dimensional profile of the radiation emissivity resulting from a tomographic inversion is shown. Radiation for the core and divertor regions is clearly indicated.

5. Improved Sensitivity of Double Layer Foil

Recent development of a new type of IRVB foil, which uses a double-layer structure has yielded a new detector which is more sensitive and stronger than the single layer IRVB [18]. This detector utilizes a stainless steel base as a supporting and thermal insulating layer to support Au or Pt absorber blocks. In Figure 4 a finite element model (FEM) comparison between the double layer foil (DLF) and the single layer IRVB foil time response to a heat source shows that the DLF is more than 3 times more sensitive. In the case of Au the increase in sensitivity is more than a factor of 10. Experimental testing of a pro-

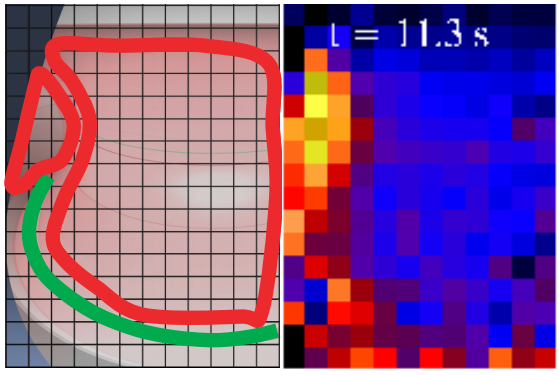

Fig. 2 a) Computer Aided Drawing of IRVB semi- tangential field of view in JT-60U with divertor region indicated by green and core region indicated by red. b) Corresponding brightness image from the IRVB in JT-60U at t = 11.3 s during shot 45664 [11].

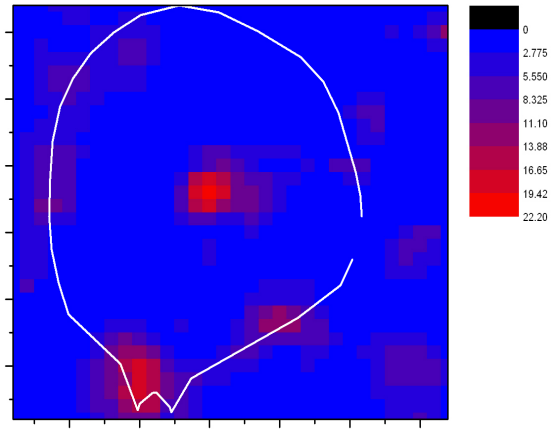

Fig. 3 Emissivity image of poloidal cross-section in JT-60U at t = 11.3 s, during shot 45664. Pixel dimension is 10 cm and white line shows the first wall.

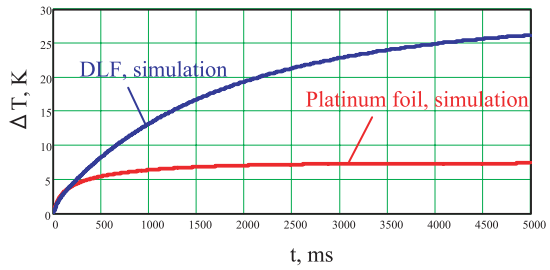

Fig. 4 Thermal response of the 10 micron Pt/2 micron stainless steel DLF and 10 micron Pt foil to the 14.7 mW/Ø 5 mm laser beam shutter opening. FEM simulation.

totype DLF has shown good agreement with the FEM results [18].

6. Upgrade of the JT-60U IRVB

In the coming year an upgrade of the IRVB on JT-60U is planned to demonstrate the ability of the IRVB to provide data useful for studies of plasma radiation and to further demonstrate its reactor relevance. In this upgrade the 2.5 μm Au foil will be replaced with a 5 μm Ta foil and the IR vacuum window diameter will be increased from 67 mm to 100 mm. The Omega IR camera will be replaced with a high performance Phoenix IR camera (see Table 1) and it will be located 2.3 m further from the machine to enable better shielding from the neutrons and magnetic field. The IR camera upgrade should improve the sensitivity of the IRVB by better than a factor of 25 as can be seen from Table 1. The increased IR throughput due to the optical upgrade, including the periscope and larger window should improve the sensitivity by a factor of approximately 2.5. If the improved shield can reduce the noise to the bit level then we can expect a further improvement in the sensitivity of around a factor of 2. In all we can expect an improvement of the sensitivity of up to a factor of 100. Using this improved sensitivity we plan to increase the number of IRVB channels by a factor of 10 (from the current 16×12 to 80×24) by reducing the size of the slit aperture form $5\,\text{mm} \times 5\,\text{mm}$ to $1\,\text{mm} \times 2.5\,\text{mm}$. This will give a spatial resolution in the divertor of 3 cm, which is equivalent to that of the existing resistive bolometers. This increase in channel number will be used to provide a more detailed tomographic inversion. In addition, with the Phoenix camera it will be possible to acquire data with 3 ms time resolution which will be adequate to distinguish individual edge localized modes albeit at lower spatial resolution.

7. Conclusions

The IRVB has been developed to the point where it is approaching the optimal noise equivalent power density of resistive bolometers of $1\,\mu\text{W/cm}^2$ at a 10 ms integration time [3]. As IR technology continues to advance IRVB sensitivity is expected to surpass this level. Tomographic techniques are being developed which allow an imaging bolometer to produce the poloidal 2D radiation emissivity data demanded by physics studies. The combination of these capabilities and the durability to a reactor environment of the materials used in the IRVB, point to its suitability for use as the main bolometer detector for a steady state fusion reactor. Existing and future installations of IRVBs on the Large Helical Device, JT-60U, KSTAR and JT-60SA will provide the experience needed to confidently design, install and operate IRVBs on future fusion reactors.

Acknowledgments

This research is supported by NIFS budgetary grant #NIFS06ULPP528 and MEXT Grants-in-Aid #16560729 and #16082207.

[1] A.W. Leonard *et al.*, Rev. Sci. Instrum. **66**, 1201 (1995).
[2] S. Konoshima *et al.*, Plasma Phys. Cont. Fusion **43**, 959 (2001).
[3] K.F. Mast *et al.*, Rev. Sci. Instrum. **62**, 744 (1991).
[4] T. Nishitani *et al.*, Fusion Eng. Des. **63-64**, 437 (2002).
[5] G.A. Wurden, B.J. Peterson and S. Sudo, Rev. Sci. Instrum. **68**, 766 (1997).
[6] B.J. Peterson, Rev. Sci. Instrum. **71**, 3696 (2000).
[7] B.J. Peterson *et al.*, Rev. Sci. Instrum. **74**, 2040 (2003).
[8] B.J. Peterson *et al.*, Rev. Sci. Instrum. **72**, 923 (2001).
[9] B.J. Peterson *et al.*, Plasma Phys. Contr. Fusion **45** 1167 (2003).
[10] S. Konoshima *et al.*, 32nd EPS Conf. on Plasma Phys. and Control. Fusion, ECA **29C**, P-4.092 (2005).
[11] B.J. Peterson *et al.*, J. Nucl. Mater. **363-365**, 412 (2007).
[12] H. Parchamy *et al.* Rev. Sci. Instrum. **77** 10E515 (2006).
[13] H. Parchamy *et al.*, Plasma Fusion Res. *in press*.
[14] B.J. Peterson *et al.*, 30th EPS Conf. on Control. Fusion and Plasma Phys. ECA **27A** P-4.067 (2003).
[15] http://www.goodfellow.com
[16] http://henke.lbl.gov/optical_constants/
[17] Y. Liu *et al.*, Plasma Fusion Res. *in press*.
[18] I. V. Miroshnikov *et al.*, *sub.* Plasma Fusion Research.